Received: 23 November 2021 | Revised: 15 March 2022 | Accepted: 18 April 2022

DOI: 10.4218/etrij.2021-0447

ORIGINAL ARTICLE

ETRI Journal WILEY

Performance analysis of SWIPT-assisted adaptive NOMA/OMA system with hardware impairments and imperfect CSI

Jing Guo | **Jin Lu** | **Xianghui Wang** | **Lili Zhou**

School of Electronic Information and Artificial Intelligence, Shaanxi University of Science and Technology, Xi'an, Shaanxi, China

Correspondence
Jing Guo, School of Electronic Information and Artificial Intelligence, Shaanxi University of Science and Technology, Xi'an, Shaanxi, China.
Email: snowy0821@163.com

Funding information
National Natural Science Foundation of China, Grant/Award Numbers: 61801281, 62171265

Abstract

This paper investigates the effect of hardware impairments (HIs) and imperfect channel state information (ICSI) on a SWIPT-assisted adaptive nonorthogonal multiple access (NOMA)/orthogonal multiple access (OMA) system over independent and nonidentical Rayleigh fading channels. In the NOMA mode, the energy-constrained near users act as a relay to improve the performance for the far users. The OMA transmission mode is adopted to avoid a complete outage when NOMA is infeasible. The best user selection scheme is considered to maximize the energy harvested and avoid error propagation. To characterize the performance of the proposed systems, closed-form and asymptotic expressions of the outage probability for both near and far users are studied. Moreover, exact and approximate expressions of the ergodic rate for near and far users are investigated. Simulation results are provided to verify our theoretical analysis and confirm the superiority of the proposed NOMA/OMA scheme in comparison with the conventional NOMA and OMA protocol with/without HIs and ICSI.

KEYWORDS

ergodic rate, hardware impairments, imperfect channel state information, nonorthogonal multiple access, outage probability, simultaneous wireless information and power transfer

1 | INTRODUCTION

Higher spectral and energy efficiency are among the key objectives of a 5G communication network. Nonorthogonal multiple access (NOMA) has recently attracted extensive research interest as one of the promising techniques. Unlike the traditional orthogonal multiple access (OMA), the main characteristic of NOMA is to serve multiple users in the same time/frequency/code domain simultaneously but with different power levels, which is an effective solution to enhance the spectrum efficiency [1]. Various studies have been conducted to investigate the performance of NOMA networks [2]. To expand the coverage and further improve the system performance, cooperative NOMA has been proposed [3,4]. One research type considers the "strong" NOMA users as relays to help the "weak" users. However, as relays, the "strong" NOMA users are threatened by power scarcity in the cooperative process. Thus, its lifetime would be shortened. Therefore, the question is how to enable NOMA users to perform the relaying operation without consuming their batteries.

Fortunately, simultaneous wireless information and power transfer (SWIPT) has been proposed as another promising technique to improve the energy efficiency of 5G networks, to prolong the lifetime of energy-constrained devices [5]. To apply SWIPT in practical scenarios, the time switching and power splitting (PS) receiver architectures [6] have been introduced, which can concurrently decode information and harvest energy from the transmitted radio frequency (RF) signals. The former processes the received signal at different times to harvest energy and decode information, whereas the latter harvests energy and decodes information by splitting the signal into two streams. The combination of SWIPT and cooperative NOMA improves the system's performance through collaborative behavior and avoids draining the batteries of the energy-constrained devices [7,8]. Several studies have proved that in the SWIPT networks, NOMA can achieve better performance than OMA by appropriately allocating transmit power and optimizing the decoding order [9]. However, under poor channel conditions, NOMA achieves a lower system capacity than OMA due to inter-user interference [10]. Moreover, the strong NOMA users are unable to act as a relay to help the weak users in the entire transmission process [11]. Therefore, it is necessary to switch between NOMA and OMA when NOMA is infeasible [12].

However, the studies above are analyzed assuming that all RF components and the channel state information (CSI) are perfect. In practice, RF transceivers always suffer from several hardware impairments (HIs), such as I/Q imbalance, quantization error, and phase noise [13]. Despite some mitigation algorithms, these impairments may still limit the system's performance. Recently, some studies have considered the HIs in SWIPT [14] and NOMA [15] networks. Additionally, imperfect CSI (ICSI) cannot be ignored in practical networks. The corresponding CSI at the transmitter may be outdated due to feedback delay, channel variations with time, or estimation error [16]. Especially for SWIPT NOMA systems, the ICSI can significantly lose the system's performance because the system encoding, decoding, and energy harvesting highly depend on the CSI quality. Therefore, the analysis of SWIPT-assisted NOMA systems with HIs and ICSI is critical. Understanding the impact of HIs and ICSI on the SWIPT-assisted NOMA systems has attracted much research interest [17].

Unlike the widely considered SWIPT NOMA systems, SWIPT-assisted adaptive NOMA/OMA communication systems have not been sufficiently analyzed yet. In particular, the impact of HIs and ICSI on SWIPT-assisted adaptive NOMA/OMA system performance has not been studied. Meanwhile, most of the studies consider independent and identically distributed fading channels. In practice, it may be more appropriate to consider independent but nonidentically distributed (i.n.i.d.) channels. Additionally, due to HIs and ICSI, successive interference cancelation (SIC) cannot be error free. There is a residual power from incompletely canceled previous symbols. This SIC error can propagate and rise with an increase in the number of simultaneously connected users [18]. Therefore, we seek to adopt the best user selection scheme to improve system performance and study whether it still brings performance gains with HIs and ICSI.

Motivated by these previous studies, in this paper, we focus on analyzing the joint effect of HIs and ICSI on a SWIPT-assisted adaptive NOMA/OMA system with user selection. A more general scenario, in which all channel links in the system are i.n.i.d. Rayleigh fading channels, is considered. In the NOMA mode, the near users employ PS receiver architecture to harvest energy and act as a decode-and-forward (DF) relay to forward the far users' signals. OMA is adopted when NOMA is infeasible. The main contributions of our work are summarized as follows:

i. We investigate the closed-form expressions of outage probabilities for both near and far users. We derived the asymptotic outage probabilities in the ideal and nonideal conditions to obtain deeper insights. The diversity orders of the near and far users are obtained. The results indicated that there is an error floor for the near users in the nonideal conditions. As the transmitting power increases, the outage performance of far users always decreases, whereas for the conventional NOMA systems, the outage performance tends to be a fixed constant in the nonideal conditions [17]. Moreover, due to the HIs and ICSI, there is no diversity gain obtained using user selection for both near and far users.
ii. The approximate expressions of ergodic rates for both near and far users are derived. From the asymptotic expression of ergodic rates, it is demonstrated that a throughput ceiling always exists for both near and far users in ideal and nonideal conditions in the high signal-to-noise ratio (SNR) region. The power allocation coefficients a_1 and a_2 play critical roles in the ergodic rates for both near and far users.
iii. Numerical results are presented to verify the correctness of our theoretical analysis. These results show how the essential system parameters, such as the transmit power, the number of near and far users, and the power allocation coefficients, influence the system performance under HIs and ICSI. Especially, these results confirm that our proposed system

always provides superior performance to the conventional NOMA and OMA systems with/without HIs and ICSI. Moreover, ICSI has a more severe impact on the system performance than HIs. Furthermore, the simulation results indicate that there is an optimal power coefficient a_1, which maximizes the ergodic rate of far users in the low SNR region.

2 | SYSTEM MODEL

Consider a downlink multiuser network composed of a source terminal $\mathcal{S}$ and two clusters of randomly deployed users, that is, K near users $\mathcal{N}_i, i=1,...,K$, and M far users $\mathcal{F}_j, j=1,...,M$, where all nodes are equipped with a single antenna and operated in a half-duplex mode. Let h_{AB} denote the channel fading coefficient between A and B, where $A \in \{\mathcal{S}, \mathcal{N}_i\}$ and $B \in \{\mathcal{N}_i, \mathcal{F}_j\}$. Assume that all channels in the system are block Rayleigh fading channels, the channel gains, $|h_{AB}|^2$, are independent and exponential random variables with means of $\lambda_{AB} = d_{AB}^{-\alpha}$, where d_{AB} is the distance between A and B, and α is the path loss exponent. Additionally, we assume that all terminals have the same zero mean additive white Gaussian noise (AWGN) with average power N_0.

This paper considers the transmission mode switching (NOMA/OMA) and the best user selection scheme in a downlink transmission scenario. Before the data transmission, $\mathcal{S}$ transmits a pilot to estimate the channel gains and accomplish the selection process. The best near and best far users are selected through their respective channel conditions. Additionally, the NOMA/OMA switching process depends on the condition of the channel link $\mathcal{S}-\mathcal{N}_i$. When $|h_{SN_i}|^2$ is not less than a given threshold, NOMA signaling is adopted, and the selected near user $\mathcal{N}_s$ is employed as a PS-based energy harvesting relay to forward signals to the selected far user $\mathcal{F}_s$; otherwise, OMA signaling is adopted.

Note that, in practice, the exact CSI is almost impossible to obtain due to complex channel environments. Furthermore, it is essential to consider the delayed CSI feedback. The time interval between user selection and data transmission may result in a certain degree of mismatch between the real value h_{AB} and the estimate $\hat{h}_{AB}$, whose relationship can be expressed as $h_{AB} = \sqrt{\varepsilon_{AB}}\hat{h}_{AB} + \sqrt{1-\varepsilon_{AB}}e_{AB}$, where $\varepsilon_{AB} \in [0,1]$ is the correlation coefficient between h_{AB} and $\hat{h}_{AB}$ [19]. A larger ε_{AB} means better CSI accuracy. e_{AB} is the zero mean and unit variance estimation error noise. We assume that $\hat{h}_{AB}$ and e_{AB} are independent.

2.1 | NOMA cooperative transmission with SWIPT

In the proposed cooperative NOMA scheme, information transmission in each block is divided into two time slots. The source or a near user is selected to transmit signal packets in each time slot, and each time slot has the same transmission period T.

2.1.1 | The first phase

Suppose that $\mathcal{N}_s$ and $\mathcal{F}_s$ have been selected for information transmission (the selection criterion will be discussed later). According to the NOMA principle, $\mathcal{S}$ transmits a superimposed signal, x_{N_s} and x_{F_s} for $\mathcal{N}_s$ and $\mathcal{F}_s$, using the powers a_1P and a_2P, respectively, where a_1 and a_2 are the power allocation coefficients, $0 < a_1 < a_2$ and $a_1 + a_2 = 1$, P is the transmit power of $\mathcal{S}$.

At the near user $\mathcal{N}_s$, the received signal can be expressed as

$$y_{SN_s} = h_{SN_s}\left(\sqrt{a_1 P}x_{N_s} + \sqrt{a_2 P}x_{F_s} + \eta_{t,S}\right) + \eta_{r,N_s} + n_{N_s}, \quad (1)$$

where n_{N_s} is the AWGN at $\mathcal{N}_s$, $\eta_{t,S} \sim \mathcal{CN}\left(0, k_{t,S}^2 P\right)$ and $\eta_{r,N_s} \sim \mathcal{CN}\left(0, k_{r,N_s}^2 P|h_{SN_s}|^2\right)$ denote the distortion noises generated by the transmitter and receiver, respectively [20].

By applying the PS-based SWIPT, the signal at $\mathcal{N}_s$ is divided into two parts with a splitting ratio ρ $(0 < \rho < 1)$. One part is used to harvest energy. Note that the noise power and the HIs have not been considered [14,21]. The energy harvested by $\mathcal{N}_s$ can be expressed as $E_{N_s} = T\eta\rho P|h_{SN_s}|^2$, where $0 < \eta < 1$ is the energy conversion efficiency. The remaining part is used for information decoding. By applying the SIC receiver, $\mathcal{N}_s$ first decodes the signal x_{F_s} and subtracts it from the superposed signal to detect its own signal x_{N_s}. Thus, at $\mathcal{N}_s$, the SNR for detecting the far user $\mathcal{F}_s$ symbols and its own symbols can be expressed as

$$\gamma_{SN_s}^F = \frac{(1-\rho)a_2\overline{\gamma}|h_{SN_s}|^2}{(1-\rho)\left(a_1 + k_{SN_s}^2\right)\overline{\gamma}|h_{SN_s}|^2 + 1}, \quad (2)$$

and

$$\gamma_{SN_s}^N = \frac{(1-\rho)a_1\overline{\gamma}|h_{SN_s}|^2}{(1-\rho)\left(a_2\varepsilon + k_{SN_s}^2\right)\overline{\gamma}|h_{SN_s}|^2 + (1-\rho)(1-\varepsilon_{SN_s})a_2\overline{\gamma} + 1}, \quad (3)$$

respectively, where $\overline{\gamma} = P/N_0$ denotes the average transmit SNR, $k_{\mathrm{SN}_s} = \sqrt{k_{t,\mathrm{S}}^2 + k_{r,\mathrm{N}_s}^2}$, and $\varepsilon = \left(1 - \sqrt{\varepsilon_{\mathrm{SN}_s}}\right)^2$ describes the residual interference due to the impact of the ICSI.

When NOMA is enabled, the PS-based SWIPT protocol first guarantees the correct detection of x_{F_s} at $\mathcal{N}_s$. Subsequently, $\mathcal{N}_s$ can harvest the remaining energy and be selected to forward x_{F_s} to $\mathcal{F}_s$. Let γ_n and γ_f denote the targeted SNR required to successfully decode the information x_{N_s} and x_{F_s}, respectively. The events $\gamma_{\mathrm{SN}_s}^F \geq \gamma_f$ must be satisfied. After some algebraic manipulations, and maximizing the energy harvested, the PS coefficient can be set as

$$\rho = \max\left\{0, 1 - \frac{\gamma_f}{\left(a_2 - \left(a_1 + k_{\mathrm{SN}_s}^2\right)\gamma_f\right)\overline{\gamma}|h_{\mathrm{SN}_s}|^2}\right\}. \quad (4)$$

We assume that all the harvested energy is used for transmitting the information from $\mathcal{N}_s$ to $\mathcal{F}_s$. Hence, the transmit power at $\mathcal{N}_s$ can be given by

$$P_{\mathrm{N}_s} = E_{\mathrm{N}_s}/T = \eta\rho P|h_{\mathrm{SN}_s}|^2. \quad (5)$$

At $\mathcal{F}_s$, the received signal can be expressed as

$$y_{\mathrm{SF}_s} = h_{\mathrm{SF}_s}\left(\sqrt{a_1 P}x_{\mathrm{N}_s} + \sqrt{a_2 P}x_{\mathrm{F}_s} + \eta_{t,\mathrm{S}}\right) + \eta_{r,\mathrm{F}_s} + n_{\mathrm{F}_s}, \quad (6)$$

where n_{F_s} is the AWGN at $\mathcal{F}_s$, and $\eta_{r,\mathrm{F}_s} \sim \mathcal{CN}\left(0, k_{r,\mathrm{F}_s}^2 P|h_{\mathrm{SF}_s}|^2\right)$ denote the distortion noise. Consequently, the SNR at $\mathcal{F}_s$ that decodes the x_{F_s} transmitted from $\mathcal{S}$ can be given by

$$\gamma_{\mathrm{SF}_s}^F = \frac{a_2\overline{\gamma}|h_{\mathrm{SF}_s}|^2}{\left(a_1 + k_{\mathrm{SF}_s}^2\right)\overline{\gamma}|h_{\mathrm{SF}_s}|^2 + 1}, \quad (7)$$

where $k_{\mathrm{SF}_s} = \sqrt{k_{t,\mathrm{S}}^2 + k_{r,\mathrm{F}_s}^2}$.

2.1.2 | The second phase

Considering the DF protocol, the received signal at $\mathcal{F}_s$ from $\mathcal{N}_s$ can be written as

$$y_{\mathrm{N}_s\mathrm{F}_s} = \sqrt{P_{\mathrm{N}_s}}h_{\mathrm{N}_s\mathrm{F}_s}\left(x_{\mathrm{F}_s} + \eta_{t,\mathrm{N}_s}\right) + \eta_{r,\mathrm{F}_s} + n_{\mathrm{F}_s}, \quad (8)$$

where $\eta_{t,\mathrm{N}_s} \sim \mathcal{CN}\left(0, k_{t,\mathrm{N}_s}^2 P_{\mathrm{N}_s}\right)$ denotes the distortion noise. Consequently, the SNR at $\mathcal{F}_s$ to decode the x_{F_s} can be given by

$$\gamma_{\mathrm{N}_s\mathrm{F}_s} = \frac{\eta\rho\overline{\gamma}|h_{\mathrm{SN}_s}|^2|h_{\mathrm{N}_s\mathrm{F}_s}|^2}{\eta\rho k_{\mathrm{N}_s\mathrm{F}_s}^2\overline{\gamma}|h_{\mathrm{SN}_s}|^2|h_{\mathrm{N}_s\mathrm{F}_s}|^2 + 1}. \quad (9)$$

where $k_{\mathrm{N}_s\mathrm{F}_s} = \sqrt{k_{t,\mathrm{N}_s}^2 + k_{r,\mathrm{F}_s}^2}$.

As in Osorio and others [22] and Yue and others [23], we assume that the near users' processing delay is much smaller than the signal block length. In other words, there is some time interval between the signals received by the far user from $\mathcal{S}$ and $\mathcal{N}_s$. Hence, these signals from $\mathcal{S}$ and $\mathcal{N}_s$ can be fully resolvable by $\mathcal{F}_s$, respectively. Then, $\mathcal{F}_s$ combines the two signals from the $\mathcal{S}$ and $\mathcal{N}_s$ by the selection combining (SC) technique.[1] Finally, the achievable SNR for detecting x_{F_s} at $\mathcal{F}_s$ can be given by

$$\gamma_{\mathrm{F}_s}^{SC} = \max\left\{\gamma_{\mathrm{SF}_s}^F, \gamma_{\mathrm{N}_s\mathrm{F}_s}\right\}. \quad (10)$$

2.1.3 | User selection scheme

According to the channel gain between $\mathcal{S}$ and $\mathcal{N}_s$, we first form a subset Q of K, in which these users can not only successfully decode both x_{N_s} and x_{F_s} but also harvest energy from the source. We selected the best near user $\mathcal{N}_s$ from the subset Q to enable the selected near user harvest more energy. Additionally, the best far user $\mathcal{F}_s$ in cluster M is selected based on their direct channel link $\mathcal{S} - \mathcal{F}_s$. Mathematically, the selected scheme can be expressed as

$$N_s = \arg\max_{i \in Q}|h_{\mathrm{SN}_i}|^2, \quad (11)$$

$$F_s = \arg\max_{j \in M}|h_{\mathrm{SF}_j}|^2, \quad (12)$$

and

$$Q = \left\{i : 1 \leq i \leq K, \overline{\gamma}|h_{\mathrm{SN}_i}|^2 - \frac{1}{v} > 0\right\}, \quad (13)$$

where $v = \left(a_2 - \left(a_1 + k_{\mathrm{SN}_s}^2\right)\gamma_f\right)/\gamma_f$.

[1] SC leads to a simple receiver structure that is a good trade-off between the diversity gain and feasible hardware. Although maximal-ratio combining (MRC) may give the optimum performance, SC gives the most superior performance. Another advantage of using the SC is that it saves more power than MRC [24]. Therefore, in this study, the SC receiver is considered at the far user.

2.2 | OMA transmission

OMA signaling is adopted if $Q=0$, for example, in time division multiple access. Each user can only occupy half of the time frame to receives their messages. Similarly, before information transmission, the best far user $\mathcal{F}_s$ and best near user $\mathcal{N}'_s$ are selected using (12) and $N'_s = \underset{i \in \mathcal{K}}{\operatorname{argmax}} |h_{\mathrm{SN}_i}|^2$, respectively. Hence, the SNR at $\mathcal{N}_s$ and $\mathcal{F}_s$ can be given by

$$\gamma_{\mathrm{N}'_s} = \frac{\overline{\gamma}|h_{\mathrm{SN}'_s}|^2}{k^2_{\mathrm{SN}_s}\overline{\gamma}|h_{\mathrm{SN}'_s}|^2+1}, \quad \gamma_{\mathrm{F}_s} = \frac{\overline{\gamma}|h_{\mathrm{SF}_s}|^2}{k^2_{\mathrm{SF}_s}\overline{\gamma}|h_{\mathrm{SF}_s}|^2+1}. \tag{14}$$

3 | PERFORMANCE ANALYSIS

3.1 | Outage probability

3.1.1 | Outage probability of the near users

In our system, an outage can occur when the near users cannot detect the signal in both the NOMA and OMA protocol. Considering independent and random channels, the outage probability of the near users can be expressed as

$$P^N_{\mathrm{out}} = \Pr\left\{\gamma_{\mathrm{N}'_s} < \gamma_n, Q=0\right\} + \Pr\left\{\gamma^N_{\mathrm{SN}_s} < \gamma_n, Q \neq 0\right\}. \tag{15}$$

The CDF $F_{h_{\mathrm{SN}'_s}}(x)$ is first analyzed to obtain the outage probability of the near users. According to Vicario and Anton-Haro [25], we have

$$f_{h_{\mathrm{SN}'_s}}(x) = \int_0^\infty f_{h_{\mathrm{SN}'_s}|\hat{h}_{\mathrm{SN}'_s}}(x|y) f_{\hat{h}_{\mathrm{SN}'_s}}(y)dy, \tag{16}$$

where

$$f_{h_{\mathrm{SN}'_s}|\hat{h}_{\mathrm{SN}'_s}}(x|y) = \frac{1}{(1-\varepsilon_{\mathrm{SN}_s})\hat{\lambda}_{\mathrm{SN}_s}} \times \exp\left(-\frac{x+\varepsilon_{\mathrm{SN}_s}y}{(1-\varepsilon_{\mathrm{SN}_s})\hat{\lambda}_{\mathrm{SN}_s}}\right) I_0\left(\frac{2\sqrt{\varepsilon_{\mathrm{SN}_s}xy}}{(1-\varepsilon_{\mathrm{SN}_s})\hat{\lambda}_{\mathrm{SN}_s}}\right), \tag{17}$$

in which $I_0(\cdot)$ is the zeroth-order modified Bessel function of the first kind [26, eq. (8.406)]. Moreover,

$$\begin{aligned} f_{\hat{h}_{\mathrm{SN}'_s}}(y) &= \frac{\partial}{\partial y} Pr\left\{\max_{i \in \mathcal{K}} \left|\hat{h}_{\mathrm{SN}_i}\right|^2 < y\right\} \\ &= \frac{\partial}{\partial y} \prod_{i=1}^{K} \left(1 - \exp\left(-\frac{y}{\hat{\lambda}_{\mathrm{SN}_i}}\right)\right) \\ &= \sum_{i,n_i} \sum_{k=1}^{i} \frac{1}{\hat{\lambda}_{\mathrm{SNn}_k}} \exp\left(-\sum_{k=1}^{i} \frac{y}{\hat{\lambda}_{\mathrm{SNn}_k}}\right). \end{aligned} \tag{18}$$

where $\sum_{i,n_i} = \sum_{i=1}^{K} (-1)^{i-1} \sum_{\substack{n_1=1 \\ n_1<n_2<\cdots<n_i}}^{K} \sum_{n_2=1}^{K} \cdots \sum_{n_i=1}^{K}$. Substituting (17) and (18) into (16), and using [27, eq. (2.15.5.4)], we obtain

$$f_{h_{\mathrm{SN}'_s}}(x) = \sum_{i,n_i} \sum_{k=1}^{i} \frac{A_{n_k}}{\hat{\lambda}_{\mathrm{SNn}_k}} \exp\left(-\sum_{k=1}^{i} \frac{A_{n_k}}{\hat{\lambda}_{\mathrm{SNn}_k}} x\right) \tag{19}$$

where $A_{n_k} = 1/\left(\varepsilon_{\mathrm{SN}_s} + (1-\varepsilon_{\mathrm{SN}_s})\hat{\lambda}_{\mathrm{SN}_s} \sum_{k=1}^{i} \frac{1}{\hat{\lambda}_{\mathrm{SNn}_k}}\right)$.

Thus, we have the CDF of $|h_{\mathrm{SN}^s_i}|^2$ as

$$F_{h_{\mathrm{SN}'_s}}(x) = 1 - \sum_{i,n_i} \exp\left(-\sum_{k=1}^{i} \frac{1}{\hat{\lambda}_{\mathrm{SNn}_k}} A_{n_k} x\right). \tag{20}$$

Next, we evaluate the CDF, $F_{h_{\mathrm{SN}_s}}(x)$. To perform further analyses, we firstly have to find the conditional CDF of $|\hat{h}_{\mathrm{SN}_s}|^2$, which is expressed as

$$F_{\hat{h}_{\mathrm{SN}_s}}(z) = \Pr\left\{\max_{i \in Q} \left|\hat{h}_{\mathrm{SN}_i}\right|^2 < z\right\}. \tag{21}$$

Actually, it is difficult to compute (21) especially when the channels are assumed to be i.n.i.d. To overcome this difficulty, we invoke the technique described in Beaulieu and Hu [28] to simplify the complexity of the calculation. In our NOMA protocol, the near user can be selected only if the event $\overline{\gamma}|h_{\mathrm{SN}_i}|^2 - (1/v) > 0$ is satisfied. As in Beaulieu and Hu [28], the PDF of $|\hat{h}_{\mathrm{SN}_i}|^2$ can be rewritten as

$$\begin{aligned} &\tilde{f}_{\hat{h}_{\mathrm{SN}_i}}(z) \\ &= f_{\hat{h}_{\mathrm{SN}_i}|i \notin Q}(x)\Pr\{i \notin Q\} + f_{\hat{h}_{\mathrm{SN}_i}|i \in Q}(x)\Pr\{i \in Q\} \\ &= B_i\delta(0) + (1-B_i)\frac{1}{\hat{\lambda}_{\mathrm{SN}_i}} \exp\left(-\frac{z}{\hat{\lambda}_{\mathrm{SN}_i}}\right), \end{aligned} \tag{22}$$

where B_i denotes the probability that the ith near user is not in the selection set, hence,

$$B_i = \Pr\left\{\overline{\gamma}|\hat{h}_{\mathrm{SN}_i}|^2 - \frac{1}{v} < 0\right\} = 1 - \exp\left(-\frac{1}{\overline{\gamma}\lambda_{\mathrm{SN}_i} v}\right). \quad (23)$$

Then, the CDF of $|\hat{h}_{\mathrm{SN}_i}|^2$ can be easily derived as

$$\tilde{F}_{\hat{h}_{\mathrm{SN}_i}}(z) = 1 - (1 - B_i)\exp\left(-\frac{z}{\hat{\lambda}_{\mathrm{SN}_i}}\right). \quad (24)$$

Now, the unconditional CDF of $|\hat{h}_{\mathrm{SN}_s}|^2$ can be given by

$$F_{\hat{h}_{\mathrm{SN}_s}}(z) = \Pr(\max_{i \in \mathcal{K}} |\hat{h}_{\mathrm{SN}_i}|^2 < z) = \prod_{i=1}^{K} \tilde{F}_{\hat{h}_{\mathrm{SN}_i}}(z). \quad (25)$$

Note that the CDF $F_{h_{\mathrm{SN}_s}}(z)$ in (21) and (25) are equal. By taking the derivative of (25) with respect to z, and applying some manipulations, we obtain the unconditional PDF of the channel gain $|\hat{h}_{\mathrm{SN}_s}|^2$ as

$$f_{\hat{h}_{\mathrm{SN}_s}}(z) = \prod_{i=1}^{K} B_i \delta(z) + \sum_{i,n_i} \prod_{k=1}^{i} (1 - B_{n_k}) \exp\left(-\frac{z}{\hat{\lambda}_{\mathrm{SNn}_k}}\right) \sum_{k=1}^{i} \frac{1}{\hat{\lambda}_{\mathrm{SNn}_k}}. \quad (26)$$

Notably, the expression of $f_{\hat{h}_{\mathrm{SN}_s}}(z)$ in (26) includes the situation where all the near users are not in the set Q. Therefore, the unconditional PDF of the channel gain $|\hat{h}_{\mathrm{SN}_s}|^2$ in our system can be expressed as

$$\begin{aligned} f'_{\hat{h}_{\mathrm{SN}_s}}(z) &= f_{\hat{h}_{\mathrm{SN}_s}}(z) - \prod_{i=1}^{K} B_i \delta(z) \\ &= \sum_{i,n_i} \prod_{k=1}^{i} (1 - B_{n_k}) \exp\left(-\frac{z}{\hat{\lambda}_{\mathrm{SNn}_k}}\right) \sum_{k=1}^{i} \frac{1}{\hat{\lambda}_{\mathrm{SNn}_k}}. \end{aligned} \quad (27)$$

Similarly, the PDF of $|h_{\mathrm{SN}_s}|^2$ is given by

$$\begin{aligned} f_{h_{\mathrm{SN}_s}}(x) &= \int_0^{\infty} f_{h_{\mathrm{SN}_s}|\hat{h}_{\mathrm{SN}_s}}(x|z) f'_{\hat{h}_{\mathrm{SN}_s}}(z) dz \\ &= \sum_{i,n_i} \prod_{k=1}^{i} (1 - B_{n_k}) \sum_{k=1}^{i} \frac{A_{n_k}}{\hat{\lambda}_{\mathrm{SNn}_k}} \exp\left(-\sum_{k=1}^{i} \frac{A_{n_k}}{\hat{\lambda}_{\mathrm{SNn}_k}} x\right), \end{aligned} \quad (28)$$

and

$$F_{h_{\mathrm{SN}_s}}(x) = 1 - \sum_{i,n_i} \prod_{k=1}^{i} (1 - B_{n_k}) \exp\left(-\sum_{k=1}^{i} \frac{A_{n_k}}{\hat{\lambda}_{\mathrm{SNn}_k}} x\right). \quad (29)$$

Using (20) and (29) in (15), the outage probability of the near users P_{out}^{N} can finally be given by

$$\begin{aligned} P_{\mathrm{out}}^{N} = {} & F_{h_{\mathrm{SN}'_s}}\left(\max\left(\frac{1}{v\overline{\gamma}}, \frac{\gamma_n}{\left(1 - k_{\mathrm{SN}_s}^2 \gamma_n\right)\overline{\gamma}}\right)\right) \\ & + F_{h_{\mathrm{SN}_s}}\left(\frac{(1 - \varepsilon_{\mathrm{SN}_s}) a_2 \gamma_n}{a_1 - \left(a_2 \varepsilon + k_{\mathrm{SN}_s}^2\right)\gamma_n - v\gamma_n}\right). \end{aligned} \quad (30)$$

Note that the equation establishes when $v > 0, k_{\mathrm{SN}_s}^2 \gamma_n < 1$ and $a_1 > \left(a_2 \varepsilon + k_{\mathrm{SN}_s}^2\right)\gamma_n + v\gamma_n$.

3.1.2 | Outage probability of the far users

With our proposed protocol, the outage events at $\mathcal{F}_s$ can occur in two cases. One is that x_{F_s} cannot be detected at $\mathcal{F}_s$ when $Q = 0$; and when $Q \neq 0$, the direct and relay links cannot detect x_{F_s} at $\mathcal{F}_s$. Therefore, the outage probability of $\mathcal{F}_s$ can be expressed as

$$P_{\mathrm{out}}^{F} = \underbrace{\Pr\left\{\gamma_{\mathrm{F}_s} < \gamma_f, Q = 0\right\}}_{P_{\mathrm{OMA}}^{F}} + \underbrace{\Pr\left\{\gamma_{\mathrm{F}_s}^{SC} < \gamma_f, Q \neq 0\right\}}_{P_{\mathrm{NOMA}}^{F}}. \quad (31)$$

Because the events $\gamma_{\mathrm{F}_s} < \gamma_f$ and $Q = 0$ are independent, P_{OMA}^{F} can be obtained as

$$\begin{aligned} P_{\mathrm{OMA}}^{F} &= \Pr\left\{\gamma_{\mathrm{F}_s} < \gamma_f\right\} \Pr\{Q = 0\} \\ &= F_{h_{\mathrm{SF}_s}}\left(\frac{\gamma_f}{\left(1 - k_{\mathrm{SF}_s}^2 \gamma_f\right)\overline{\gamma}}\right) F_{h_{\mathrm{SN}'_s}}\left(\frac{1}{\overline{\gamma} v}\right), \end{aligned} \quad (32)$$

where

$$F_{h_{\mathrm{SF}_s}}(x) = 1 - \sum_{j,n_j} \exp\left(-\sum_{m=1}^{j} \frac{C_{n_m}}{\hat{\lambda}_{\mathrm{SFn}_m}} x\right). \quad (33)$$

This can be computed in a similar fashion as $F_{h_{\mathrm{SN}_s}}(x)$, in which $\sum_{j,n_j} = \sum_{j=1}^{M} (-1)^{j-1} \sum_{n_1=1}^{M} \sum_{\substack{n_2=1 \\ n_1 < n_2 < \cdots < n_j}}^{M} \cdots \sum_{n_j=1}^{M}$, and $C_{n_m} = 1/\left(\varepsilon_{\mathrm{SF}_s} + (1 - \varepsilon_{\mathrm{SF}_s})\hat{\lambda}_{\mathrm{SF}_s} \sum_{m=1}^{j} (1/\hat{\lambda}_{\mathrm{SFn}_m})\right)$.

Additionally, we have the CDF of $|\hat{h}_{\mathrm{N}_s\mathrm{F}_s}|^2$ as

$$\begin{aligned} F_{\hat{h}_{\mathrm{N}_s\mathrm{F}_s}}(z) &= \Pr\left(\left|\hat{h}_{\mathrm{N}_s\mathrm{F}_s}\right|^2 < z\right) \\ &= \sum_{i=1}^{K}\sum_{j=1}^{M}\Pr(\mathrm{N}_s=\mathrm{N}_i)\Pr(\mathrm{F}_s=\mathrm{F}_j)F_{\hat{h}_{\mathrm{N}_i\mathrm{F}_j}}(z) \\ &= 1-\sum_{i=1}^{K}\sum_{j=1}^{M}\frac{1}{KM}\exp\left(-\frac{z}{\hat{\lambda}_{\mathrm{N}_i\mathrm{F}_j}}\right). \end{aligned} \tag{34}$$

Then, the CDF of $|h_{\mathrm{N}_s\mathrm{F}_s}|^2$ can be obtained as

$$\begin{aligned} F_{h_{\mathrm{N}_s\mathrm{F}_s}}(x) = 1-\sum_{i=1}^{K}\sum_{j=1}^{M}\frac{1}{KM} \\ \times\exp\left(-\frac{x}{(1-\varepsilon_{\mathrm{N}_s\mathrm{F}_s})\hat{\lambda}_{\mathrm{N}_s\mathrm{F}_s}+\varepsilon_{\mathrm{N}_s\mathrm{F}_s}\hat{\lambda}_{\mathrm{N}_i\mathrm{F}_j}}\right). \end{aligned} \tag{35}$$

Now, the second term of (31) can be given by

$$\begin{aligned} P^F_{\mathrm{NOMA}} = \Pr\left\{|h_{\mathrm{SF}_s}|^2 < \frac{\gamma_f}{\left(a_2-\left(a_1+k^2_{\mathrm{SF}_s}\right)\gamma_f\right)\overline{\gamma}}\right\} \\ \times\Pr\left\{\eta\left(1-k^2_{\mathrm{N}_s\mathrm{F}_s}\gamma_f\right)\left(\overline{\gamma}|h_{\mathrm{SN}_s}|^2-\frac{1}{v}\right)|h_{\mathrm{N}_s\mathrm{F}_s}|^2<\gamma_f\right\}. \end{aligned} \tag{36}$$

We let $Z=\alpha\left(\overline{\gamma}|h_{\mathrm{SN}_s}|^2-\frac{1}{v}\right)|h_{\mathrm{N}_s\mathrm{F}_s}|^2$, where $\alpha=\eta\left(1-k^2_{\mathrm{N}_s\mathrm{F}_s}\gamma_f\right)$. Applying (29), (35), and [26, eq. (3.471.9)], the CDF of Z can be given by

$$\begin{aligned} F_Z(z) &= \Pr\left\{\alpha\left(\overline{\gamma}|h_{\mathrm{SN}_s}|^2-\frac{1}{v}\right)|h_{\mathrm{N}_s\mathrm{F}_s}|^2<z\right\} \\ &= 1-F_{h_{\mathrm{SN}_s}}\left(\frac{1}{v\overline{\gamma}}\right) \quad -\sum_{i,n_i}\sum_{p=1}^{K}\sum_{q=1}^{M}\frac{2}{KM}\prod_{k=1}^{i}(1-B_{n_k}) \\ &\times\left(\sum_{k=1}^{i}\frac{A_{n_k}z}{\alpha\left((1-\varepsilon_{\mathrm{N}_s\mathrm{F}_s})\hat{\lambda}_{\mathrm{N}_s\mathrm{F}_s}+\varepsilon_{\mathrm{N}_s\mathrm{F}_s}\hat{\lambda}_{\mathrm{N}_p\mathrm{F}_q}\right)\hat{\lambda}_{\mathrm{SNn}_k}\overline{\gamma}}\right)^{\frac{1}{2}} \\ &\times\exp\left(-\sum_{k=1}^{i}\frac{A_{n_k}}{\hat{\lambda}_{\mathrm{SNn}_k}v\overline{\gamma}}\right) \\ &\times\mathcal{K}_1\left(2\sqrt{\sum_{k=1}^{i}\frac{A_{n_k}z}{\alpha\left((1-\varepsilon_{\mathrm{N}_s\mathrm{F}_s})\hat{\lambda}_{\mathrm{N}_s\mathrm{F}_s}+\varepsilon_{\mathrm{N}_s\mathrm{F}_s}\hat{\lambda}_{\mathrm{N}_p\mathrm{F}_q}\right)\hat{\lambda}_{\mathrm{SNn}_k}\overline{\gamma}}}\right), \end{aligned} \tag{37}$$

where $\mathcal{K}_1(\cdot)$ denotes the first-order modified Bessel function of the second kind [26, eq. (8.407.1)].

Finally, combining (32) and (36), the outage probability of the far users can be obtained as

$$\begin{aligned} P^F_{\mathrm{out}} = \ & F_{h_{\mathrm{SN}'_s}}\left(\frac{1}{v\overline{\gamma}}\right)F_{h_{\mathrm{SF}_s}}\left(\frac{\gamma_f}{\left(1-k^2_{\mathrm{SF}_s}\gamma_f\right)\overline{\gamma}}\right) \\ &+F_{h_{\mathrm{SF}_s}}\left(\frac{\gamma_f}{\left(a_2-\left(a_1+k^2_{\mathrm{SF}_s}\right)\gamma_f\right)\overline{\gamma}}\right)F_Z\left(\gamma_f\right). \end{aligned} \tag{38}$$

Note that the equation establishes when $k^2_{\mathrm{SF}_s}\gamma_f<1$ and $a_2>\left(a_1+k^2_{\mathrm{SF}_s}\right)\gamma_f$.

3.2 | Asymptotic outage probability

To gain better insights and ease the computation, the asymptotic analysis are studied at high SNR regimes ($\overline{\gamma}\to\infty$). With the equations $e^x\approx 1+x$ and $\mathcal{K}_1(x)=1/x+(x/2)\log(2/x)$ as x goes to 0, the asymptotic outage probabilities for near and far users are given by

$$\begin{aligned} P^N_{\mathrm{out}} \approx 1-\sum_{i,n_i}\sum_{k=1}^{i} \\ \times\exp\left(-\frac{A_{n_k}(1-\varepsilon_{\mathrm{SN}_s})a_2\gamma_n}{\hat{\lambda}_{\mathrm{SNn}_k}\left(a_1-\left(a_2\varepsilon+k^2_{\mathrm{SN}_s}\right)\gamma_n-v\gamma_n\right)}\right), \end{aligned} \tag{39}$$

and

$$\begin{aligned} P^F_{\mathrm{out}} \approx \ & \sum_{i,n_i}\sum_{j,n_j}\sum_{m=1}^{j}\sum_{p=1}^{K}\sum_{q=1}^{M}\frac{C_{n_m}}{KM\hat{\lambda}_{\mathrm{SFn}_m}} \\ &\times\frac{\gamma_f}{\left(a_2-\left(a_1+k^2_{\mathrm{SF}_s}\right)\gamma_f\right)}\frac{\theta_i}{\overline{\gamma}^2}\log\left(\frac{\overline{\gamma}}{\theta_i}\right), \end{aligned} \tag{40}$$

where $\theta_i=\sum_{k=1}^{i}\left(A_{n_k}\gamma_f/\alpha\left((1-\varepsilon_{\mathrm{N}_s\mathrm{F}_s})\hat{\lambda}_{\mathrm{N}_s\mathrm{F}_s}+\varepsilon_{\mathrm{N}_s\mathrm{F}_s}\hat{\lambda}_{\mathrm{N}_p\mathrm{F}_q}\right)\hat{\lambda}_{\mathrm{SNn}_k}\right)$.

In the special case of the absence of the HIs and ICSI, that is, $k_{\mathrm{AB}}=0$ and $\varepsilon_{\mathrm{AB}}=1$, where $A\in\{\mathcal{S},\mathcal{N}_i\}$ and $B\in\{\mathcal{N}_i,\mathcal{F}_j\}$, the asymptotic outage expressions for the near users and the far users can be further approximated as

$$P^N_{\mathrm{out}}\approx\prod_{i=1}^{K}\frac{1}{\lambda_{\mathrm{SN}_i}}\quad\max\quad\frac{\gamma_f}{a_2-a_1\gamma_f},\gamma_n\Bigg)\Bigg)^K\frac{1}{\overline{\gamma}^K}, \tag{41}$$

and

$$P_{\text{out}}^{F} \approx \begin{cases} \sum_{i,n_i}\sum_{p=1}^{K}\sum_{q=1}^{M}\prod_{j=1}^{M}\dfrac{\gamma_f^{M+1}\sum_{i=1}^{k}\frac{1}{\lambda_{\text{SNn}_i}}}{KM\eta\lambda_{\text{SF}_j}\lambda_{\text{N}_p\text{F}_q}\mu^{M}}\dfrac{1}{\overline{\gamma}^{M+1}}, & \mu>0, \\ \sum_{i,n_i}\sum_{p=1}^{K}\sum_{q=1}^{M}\dfrac{\gamma_f\sum_{i=1}^{k}\frac{1}{\lambda_{\text{SNn}_i}}}{KM\eta\lambda_{\text{N}_p\text{F}_q}}\dfrac{1}{\overline{\gamma}}, & \mu<0, \end{cases} \tag{42}$$

where $\mu = a_2 - a_1\gamma_f$.

It can be observed that the diversity gain attained by the near and far users are K and $M+1$, respectively, when there are no HIs and ICSI ($\varepsilon_{\text{AB}}=1$ and $k_{\text{AB}}=0$, for $A\in\{\mathcal{S},\mathcal{N}_i\}$ and $B\in\{\mathcal{N}_i,\mathcal{F}_j\}$). However, when $\varepsilon_{\text{AB}}\neq 1$ and $k_{\text{AB}}\neq 0$, because an error floor appears in the high SNR region, the diversity gain of the near users reduces to zero. The asymptotic outage probability of the far users depends on $\overline{\gamma}^{-2}\log\overline{\gamma}$; there is no diversity advantage of using user selection due to the ICSI and HIs.

3.3 | Ergodic rate

3.3.1 | Ergodic rate of x_{N_s}

In our considered system, x_{N_s} can be detected at the selected near user successfully in both the NOMA and OMA modes. Because the weakest link determines the capacity of the near users, the achievable rate of x_{N_s} can be written as

$$C_{\text{N}} = \frac{1}{2}\log\left(1+\min\left\{\gamma_{\text{SN}_s}^{N},\gamma_{\text{N}_s'}\right\}\right). \tag{43}$$

- Considering the HIs and ICSI ($k_{\text{AB}}\neq 0$ and $\varepsilon_{\text{AB}}\neq 1$)
  It is clear that the closed-form expression of ergodic rate for x_{N_s} is difficult to obtain under the HIs and ICSI. Instead, we provide an approximate expression for C_{N}. At high SNR, $\overline{\gamma}\to\infty, \min\left\{\gamma_{\text{SNS}}^{N},\gamma_{\text{N}_s'}\right\} \approx \min\left\{\frac{a_1|h_{\text{SN}_S}|^2}{\left(a_2\varepsilon+k_{\text{SN}_S}^2+v\right)|h_{\text{SN}_S}|^2+a_2\left(1-\varepsilon_{\text{SN}_S}\right)}, \frac{1}{k_{\text{SN}_S}^2}\right\}$. We let $W = \frac{a_1|h_{\text{SN}_S}|^2}{\left(a_2\varepsilon+k_{\text{SN}_S}^2+v\right)|h_{\text{SN}_S}|^2+a_2\left(1-\varepsilon_{\text{SN}_S}\right)}$, and the CDF $F_W(x) = F_{h_{\text{SN}_s'}}\left(\frac{(1-\varepsilon_{\text{SN}_s})a_2x}{a_1-\left(a_2\varepsilon+k_{\text{SN}_s}^2+v\right)x}\right)$, when $a_1 > \left(a_2\varepsilon+k_{\text{SN}_s}^2+v\right)x$. Then, the corresponding ergodic rate of x_{N_s} can be obtained as

$$\begin{aligned} C_{\text{N}}^{nid} &= \frac{1}{2}\left(\int_0^{\frac{1}{k_{\text{SN}_S}^2}}\log(1+x)\,f_W(x)dx + \int_{\frac{1}{k_{\text{SN}_S}^2}}^{\infty}\log\left(1+\frac{1}{k_{\text{SN}_s}^2}\right)f_W(x)dx\right) \\ &= \frac{1}{2\ln 2}\int_0^{\frac{1}{k_{\text{SN}_S}^2}}\frac{1-F_W(x)}{1+x}dx = \frac{1}{2\ln 2}\int_0^{u}\sum_{i,n_i}\exp \\ &\quad\times\left(-\sum_{k=1}^{i}\frac{A_{n_k}}{\hat{\lambda}_{\text{SNn}_k}}\frac{(1-\varepsilon_{\text{SN}_s})a_2x}{a_1-\left(a_2\varepsilon+k_{\text{SN}_s}^2+v\right)x}\right)\frac{1}{1+x}dx \end{aligned} \tag{44}$$

where $u = \min\left\{a_1/\left(a_2\varepsilon+k_{\text{SN}_s}^2+v\right), 1/k_{\text{SN}_S}^2\right\}$. Note that although the closed-form expression of C_{N}^{nid} cannot be obtained, it can also be effectively estimated via the expression (44).

- No HIs and ICSI ($k_{\text{AB}}=0$ and $\varepsilon_{\text{AB}}=1$)
  Substituting (3), (4), and (14), when $\varepsilon_{\text{AB}}=1$ and $k_{\text{AB}}=0$, the ergodic rate of x_{N_s} can be given by

$$C_{\text{N}}^{id} = \frac{1}{2}\log\left(1+\min\left\{\frac{a_1\gamma_f}{a_2-a_1\gamma_f}.\overline{\gamma}|h_{\text{SN}_s}|^2\right\}\right). \tag{45}$$

For further calculation, we let $X = \overline{\gamma}|h_{\text{SN}_s}|^2$, then, the CDF of X can be given by $F_X(x) = \prod_{i=1}^{K}(1-\exp(-x/\lambda_{\text{SN}_i}\overline{\gamma}))$. The corresponding ergodic rate of x_{N_s} under the ideal case can be obtained as (46) by using [26, eq. (3.352.1)],

$$\begin{aligned} C_{\text{N}}^{id} &= \frac{1}{2}\left(\int_0^{\frac{a_1\gamma_f}{a_2-a_1\gamma_f}}\log(1+x)f_X(x)dx + \int_{\frac{a_1\gamma_f}{a_2-a_1\gamma_f}}^{\infty}\log\left(1+\frac{a_1\gamma_f}{a_2-a_1\gamma_f}\right)f_X(x)dx\right) \\ &= \frac{1}{2\ln 2}\int_0^{\frac{a_1\gamma_f}{a_2-a_1\gamma_f}}\frac{1-F_X(x)}{1+x}dx = \frac{1}{2\ln 2}\sum_{i,n_i}e^{\sum_{i=1}^{k}\frac{1}{\lambda_{\text{SNn}_i}\overline{\gamma}}} \\ &\quad\left[\text{Ei}\left(-\sum_{i=1}^{k}\frac{1}{\lambda_{\text{SNn}_i}\overline{\gamma}}\left(\frac{a_1\gamma_f}{a_2-a_1\gamma_f}+1\right)\right)-\text{Ei}\left(-\sum_{i=1}^{k}\frac{1}{\lambda_{\text{SNn}_i}\overline{\gamma}}\right)\right], \end{aligned} \tag{46}$$

where $E(\cdot)$ denotes the expectation of the input random entity and $\text{Ei}(\cdot)$ denotes the exponential integral function [26, eq. (8.211.1)]. Moreover, because

$\lim_{x\to 0}\mathrm{Ei}(x)=\mathcal{C}+\ln(-x)$, when $x<0$, where $\mathcal{C}$ is the Euler gamma constant [26, eq. (8.214.1)], hence, in the high SNR regime $\overline{\gamma}\to\infty$, the ergodic rate can be further approximated as

$$C_{\mathrm{N}}^{id}\approx\frac{1}{2}\sum_{i,n_i}e^{\sum_{i=1}^{k}\frac{1}{\lambda_{\mathrm{SNn}_i}\overline{\gamma}}}\log\left(1+\frac{a_1\gamma_f}{a_2-a_1\gamma_f}\right). \tag{47}$$

Note that, from (47), the ergodic rate of near users can be increased by increasing K. However, when $\overline{\gamma}\to\infty, e^{\sum_{i=1}^{k}\frac{1}{\lambda_{\mathrm{SNn}_i}\overline{\gamma}}}\to 1$, the impact of K becomes unimportant. Therefore, the ergodic rate cannot be further enhanced either by increasing K or $\overline{\gamma}$. The ergodic rate is mainly affected by the parameters a_1, a_2, and γ_f.

3.3.2 | Ergodic rate of x_{F_s}

Because both $\mathcal{N}_s$ and $\mathcal{F}_s$ are capable of detecting x_{F_s} successfully, the achievable rate of x_{F_s} can be written as

$$C_{\mathrm{F}}=\frac{1}{2}\log\left(1+\min\left\{\gamma_{\mathrm{SN}_s}^{F},\gamma_{\mathrm{F}_s}^{SC},\gamma_{\mathrm{F}_s}\right\}\right). \tag{48}$$

- Considering HIs and ICSI($k_{\mathrm{AB}}\neq 0$ and $\varepsilon_{\mathrm{AB}}\neq 1$)
  At high SNR, $\min\{\gamma_{\mathrm{SN}_s}^{F},\gamma_{\mathrm{F}_s}^{SC},\gamma_{\mathrm{F}_s}\}\sim\min\{a_2/(a_1+k_{\mathrm{SN}_s}^2+v),\max\{a_2/(a_1+k_{\mathrm{SN}_s}^2),\gamma_{\mathrm{N}_s\mathrm{F}_s}\},1/k_{\mathrm{SF}_s}^2\}$. We denote $f_{\gamma_{\mathrm{N}_s\mathrm{F}_s}}(x)$ as the PDF of $\gamma_{\mathrm{N}_s\mathrm{F}_s}$. Therefore, the ergodic rate of x_{F_s} under the nonideal case can be obtained using (49):

$$\begin{aligned}C_{\mathrm{F}}^{nid}&=\frac{1}{2}\log\left(1+\min\left\{\frac{a_2}{a_1+k_{\mathrm{SN}_s}^2+v},\max\left\{\frac{a_2}{a_1+k_{\mathrm{SN}_s}^2},\gamma_{\mathrm{N}_s\mathrm{F}_s}\right\},\frac{1}{k_{\mathrm{SF}_s}^2}\right\}\right)\\&=\frac{1}{2}\left(\int_0^{\frac{a_2}{a_1+k_{\mathrm{SN}_s}^2}}\log\left(1+\min\left\{\frac{a_2}{a_1+k_{\mathrm{SN}_s}^2+v},\frac{1}{k_{\mathrm{SF}_s}^2}\right\}\right)f_{\gamma_{\mathrm{N}_s\mathrm{F}_s}}(x)dx\right.\\&\quad\left.+\int_{\frac{a_2}{a_1+k_{\mathrm{SN}_s}^2}}^{\infty}\log\left(1+\min\left\{\frac{a_2}{a_1+k_{\mathrm{SN}_s}^2+v},\frac{1}{k_{\mathrm{SF}_s}^2}\right\}\right)f_{\gamma_{\mathrm{N}_s\mathrm{F}_s}}(x)dx\right)\\&=\frac{1}{2}\log\left(1+\min\left\{\frac{a_2}{a_1+k_{\mathrm{SN}_s}^2+v},\frac{1}{k_{\mathrm{SF}_s}^2}\right\}\right),\end{aligned} \tag{49}$$

where $a_2>(a_1+k_{\mathrm{SN}_s}^2)\gamma_f$ is required to hold for (49).

- No HIs and ICSI ($k_{\mathrm{AB}}=0$ and $\varepsilon_{\mathrm{AB}}=1$)
  At high SNR, $\min\left\{\gamma_{\mathrm{SN}_s}^{F},\gamma_{\mathrm{F}_s}^{SC},\gamma_{\mathrm{F}_s}\right\}\sim\min\{a_2/a_1,\max\{Y,a_2/a_1\},V\}$, where $Y=\eta\left(\overline{\gamma}|h_{\mathrm{SN}_s}|^2-\gamma_f/\left(a_2-a_1\gamma_f\right)\right)|h_{\mathrm{N}_s\mathrm{F}_s}|^2$, let $f_Y(y)$ be the PDF of Y, $V=\overline{\gamma}|h_{\mathrm{SF}_s}|^2$, and the CDF of V is $F_V(x)=\prod_{j=1}^{M}\left(1-\exp\left(-\frac{x}{\lambda_{\mathrm{SN}_i}\overline{\gamma}}\right)\right)$. Therefore, the ergodic rate of x_{F_s} can given by

$$\begin{aligned}C_{\mathrm{F}}^{id}&=\frac{1}{2}\left(\int_0^{\frac{a_2}{a_1}}f_Y(y)dy+\int_{\frac{a_2}{a_1}}^{\infty}f_Y(y)dy\right)\\&\quad\left(\int_{\frac{a_2}{a_1}}^{\infty}\log\left(1+\frac{a_2}{a_1}\right)f_V(x)dx+\int_0^{\frac{a_2}{a_1}}\log(1+x)f_V(x)dx\right)\\&=\frac{1}{2\ln 2}\int_0^{\frac{a_2}{a_1}}\frac{1-F_V(x)}{1+x}dx=\frac{1}{2\ln 2}\sum_{j,n_j}e^{\sum_{m=1}^{j}\frac{1}{\lambda_{\mathrm{SFn}_m}\overline{\gamma}}}\\&\quad\left[\mathrm{Ei}\left(-\sum_{m=1}^{j}\frac{1}{\lambda_{\mathrm{SFn}_m}\overline{\gamma}}\left(\frac{a_2}{a_1}+1\right)\right)-\mathrm{Ei}\left(-\sum_{m=1}^{j}\frac{1}{\lambda_{\mathrm{SFn}_m}\overline{\gamma}}\right)\right].\end{aligned} \tag{50}$$

Similarly, the approximate expression of the ergodic rate for the far users under the ideal case can be obtained as

$$C_{\mathrm{F}}^{id}\approx\frac{1}{2}\sum_{j,n_j}e^{\sum_{m=1}^{j}\frac{1}{\lambda_{\mathrm{SFn}_m}\overline{\gamma}}}\log\left(1+\frac{a_2}{a_1}\right). \tag{51}$$

From (51), we observe that the number of far users M and the parameter a_2 positively impact the ergodic rate for the far users. Similarly, when $\overline{\gamma}\to\infty, e^{\sum_{m=1}^{j}(1/\lambda_{\mathrm{SFn}_m}\overline{\gamma})}\to 1$, the number of far users M becomes unimportant in the ergodic rate, and the ergodic rate is only related to the parameters a_1 and a_2.

4 | SIMULATION RESULTS

In this section, we numerically verify the accuracy of our analytical results. For simplicity, throughout the simulations, we assume that the channel gains of $\mathcal{S}-\mathcal{N}_i, \mathcal{S}-\mathcal{F}_j$, and $\mathcal{N}_i-\mathcal{F}_j$ have the same mean values, that is, $\lambda_{\mathrm{SN}_i}=\lambda_{\mathrm{SN}}, \lambda_{\mathrm{SF}_j}=\lambda_{\mathrm{SF}}$, and $\lambda_{\mathrm{N}_i\mathrm{F}_j}=\lambda_{\mathrm{NF}}, i=1,2,\ldots,K$

and $j = 1, 2, ..., M$, and $\varepsilon_{SN_i} = \varepsilon_{SF_j} = \varepsilon_{N_iF_j} = \xi$ and $k_{SN_i} = k_{SF_j} = k_{N_iF_j} = k$. Unless otherwise stated, we consider a two-dimensional topology, the distances between $\mathcal{S} - \mathcal{N}_s, \mathcal{S} - \mathcal{F}_s$, and $\mathcal{N}_s - \mathcal{F}_s$ are $d_{SN} = d, d_{SF} = 3d$, and $d_{NF} = 2.5d$, respectively, where $d = 0.5$ [29]. Moreover, we set the path loss exponent $\alpha_{SN} = \alpha_{SF} = \alpha_{NF} = 2$, the target data rate $R_N = R_F = 1$ bps/Hz, the power allocation coefficients $a_1 = 0.3, a_2 = 0.7$, and the energy conversion efficiency $\eta = 0.75$.

Figure 1 illustrates the outage probabilities of $\mathcal{N}_s$ and $\mathcal{F}_s$ versus $\bar{\gamma}$ for the different numbers of the near and far users in two conditions, that is, nonideal condition ($\xi = 0.95, k = 0.1$) and ideal condition ($\xi = 1, k = 0$). It can be observed that, for the near and far users, a significant outage performance gain can be achieved by increasing K and M. Additionally, for the near users, the proposed NOMA/OMA adaptive system is always superior to NOMA under ideal conditions. When $\xi = 0.95, k = 0.1$, there are error floors at high SNR, which is consistent with the discussions on the outage probability for the near users in Section 3. For the far users, we can observe that the performance of the proposed NOMA/OMA scheme exceeds that of NOMA and OMA for all SNR regions with/without HIs and ICSI.

Figure 2 shows the outage probability of $\mathcal{N}_s$ and $\mathcal{F}_s$ versus $\bar{\gamma}$ with different nonideal factors. To quantify the influence of the HIs and ICSI, we examine the outage probabilities of the near and far users in three different cases: $\xi = 0.95, k = 0$; $\xi = 1, k = 0.1$; and $\xi = 1, k = 0$. One can observe that the outage performance of the near and far users decreases when ξ increases and k decreases. When the HIs exist, the outage probabilities of both near and far users can improve with the increase of SNR. With $\xi = 1, k = 0.1$ and $\xi = 1, k = 0$, the near and far users can achieve full diversity order (i.e., K and $M+1$), respectively. This means that HIs only reduce the coding gain. When the ICSI exists, the diversity order of the near users equals zero at the high SNR region, and the diversity order achieved by $\mathcal{F}_s$ is reduced to $\bar{\gamma}^{-2}\log\bar{\gamma}$. Hence, we can conclude that the ICSI has a more severe impact on the system performance than HIs.

Figure 3 shows the outage performance of users versus the ICSI parameter ξ with different k when $\bar{\gamma} = 20$ dB. We can see that a lower channel estimation accuracy results in a higher outage for the near users than the far users with the same value of k. And the outage performance of near users is more insensitive to the channel estimation accuracy than that of far users. This is because the ICSI will reduce the users' diversity gain and lead to the SIC error, which impacts the performance of the near users and has no effect on the far users. Additionally, we

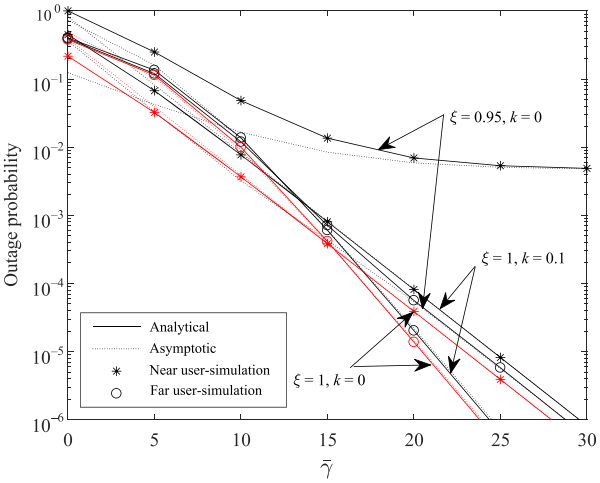

FIGURE 2 Outage probability of $\mathcal{F}_s$ versus SNR with different nonideal factors

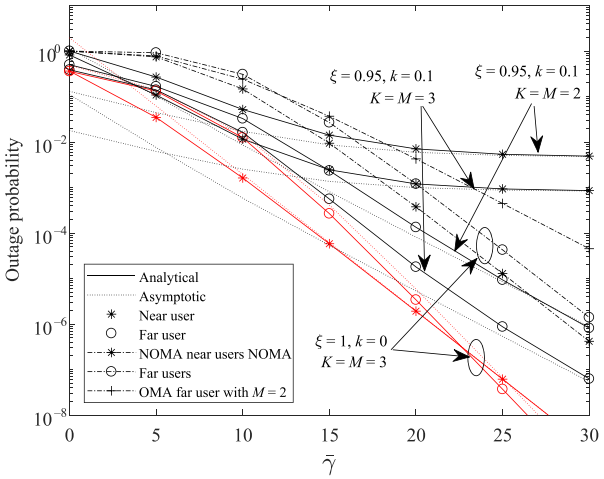

FIGURE 1 Outage probability of $\mathcal{N}_s$ and $\mathcal{F}_s$ versus $\bar{\gamma}$ with different K and M

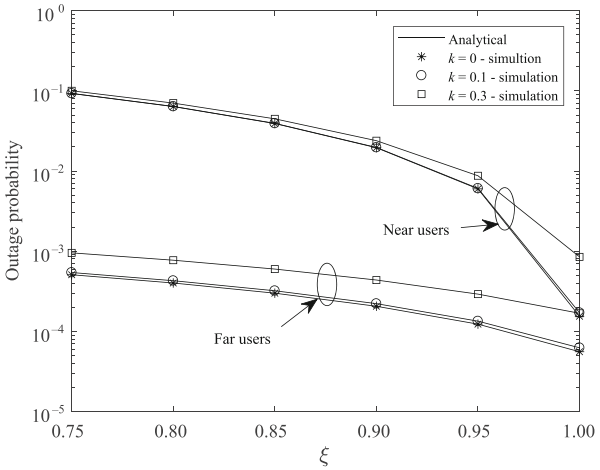

FIGURE 3 Outage performance of users versus the ICSI parameter ξ with different k

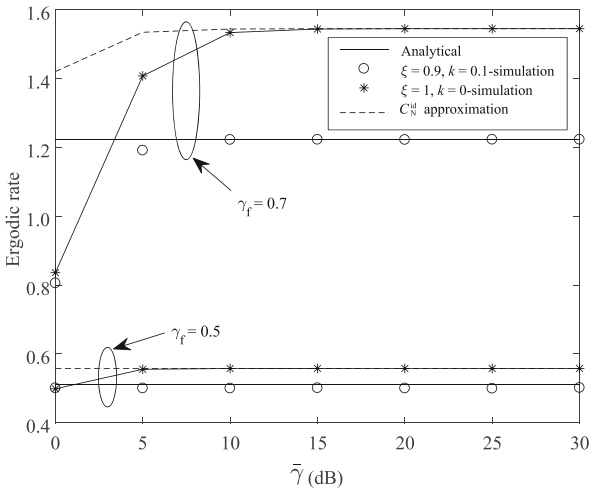

FIGURE 4 Ergodic rate of $\mathcal{N}_s$ versus $\overline{\gamma}$ with different γ_f

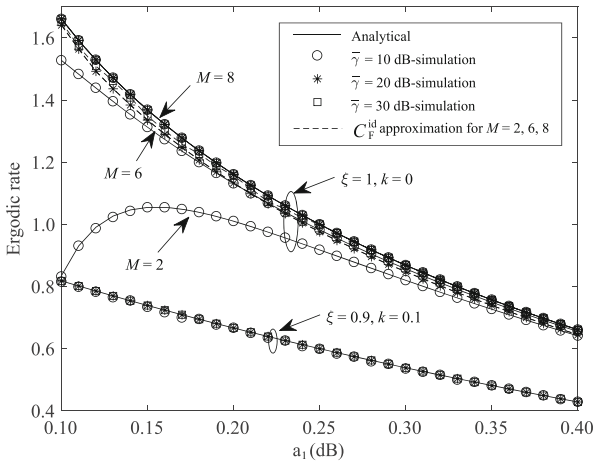

FIGURE 5 Ergodic rate of $\mathcal{F}_s$ versus a_1 with different $\overline{\gamma}$ and M

can observe that the outage performance for the far users degrades significantly when the HIs level k increases from 0 to 0.3, whereas the performance loss of the near users caused by the HIs is slightly less with k increasing when $\xi \neq 1$. This result shows that the effect of ICSI on the outage performance of near users is more severe than that of HIs.

Figure 4 shows the ergodic rates of $\mathcal{N}_s$ versus $\overline{\gamma}$ for different γ_f under ideal and nonideal conditions, that is, $\xi = 1, k = 0$ and $\xi = 0.9, k = 0.1$. It can be observed that the analytical and simulation results match well with each other, and the approximate analyses are more valid in the high SNR regime. It can be seen that the ergodic rate of the near users can be improved by increasing ξ and decreasing k. Moreover, we can see that there is a throughput ceiling as $\overline{\gamma}$ increases in both the ideal and nonideal conditions. One can observe that the ergodic rate of the near users increases with the increase of the required rate γ_f. This is because, in our proposed NOMA/OMA protocol, after decoding the signal correctly, $\mathcal{N}_s$ should maximize the collection of energy as much as possible. Therefore, under the premise of ensuring the correct decoding, the remaining power is allocated to $\mathcal{N}_s$ for the energy harvested rather than for performance improvement. Moreover, the ergodic rate is achieved faster as $\overline{\gamma}$ increases when the set value γ_f is lower, that is, $\gamma_f = 0.5$.

Figure 5 shows the ergodic rates of $\mathcal{F}_s$ versus a_1 for different $\overline{\gamma}$ and M. The figure shows that the asymptotic ergodic rate expression can considerably approximate the simulation results in both the ideal and nonideal conditions. In the ideal conditions, it can be observed that the ergodic rates of $\mathcal{F}_s$ can increase as $\overline{\gamma}$ or M increases. However, the performance gain were negligible when M increases from 6 to 8 and $\overline{\gamma}$ increases from 20 to 30 dB. This is consistent with the approximate results of (51); the ergodic rate saturates when $\overline{\gamma}$ is very high. The ergodic rate cannot be further enhanced by increasing $\overline{\gamma}$ or the number of far users M. Moreover, we can observe that there is an optimal value a_1 when $\overline{\gamma}$ is low, thta is, $\overline{\gamma} = 10$ dB. The reason is that a_1 indicates the trade-off between the near and far users to decode their signals correctly. Because the channel condition of link $\mathcal{S} - \mathcal{N}_s$ is better than that of link $\mathcal{S} - \mathcal{F}_s$, on increasing $\overline{\gamma}$, less power (a smaller a_1) for $\mathcal{N}_s$ is sufficient for decoding its own signal. Hence, more energy can be allocated to the far users to improve their performance. However, in the nonideal conditions, the ergodic rates of $\mathcal{F}_s$ remain unchanged with an increase in $\overline{\gamma}$, which shows that the performance of the far users cannot be improved by simply increasing the SNR. This is because, when $\overline{\gamma} \to \infty$, the ergodic rates of $\mathcal{F}_s$ is only related to a_1 and a_2.

5 | CONCLUSION

In this paper, we studied the impact of the HIs and ICSI on the performance of a SWIPT-assisted adaptive NOMA/OMA system. The closed-form and asymptotic expressions for the outage probabilities of both near and far users were derived over the i.n.i.d. Rayleigh fading channels. The diversity gains attained by the near and far users are K and $M+1$ in the ideal conditions, respectively. However, the performance of the near and far users declined when the HIs and ICSI existed, and the diversity gains achieved by the near and far users were reduced to zero and $\overline{\gamma}^{-2}\log\overline{\gamma}$, respectively. Moreover, the ergodic rates of the near and far users were studied to gain further insight into the effect of the system's important parameters. The results have shown that there is a throughput ceiling of the ergodic rates for both near and

far users in the ideal and nonideal conditions, which means that the system performance will not be further improved with an increase in SNR. Analytical and numerical results demonstrated that, whether the HIs and ICSI exist or not, our proposed adaptive NOMA/OMA system with SWIPT obtains better performance than the conventional NOMA and OMA system. The effect of the ICSI on the performance of the near users is more serious than that of HIs. In the ideal condition, the ergodic rate of the near users mainly depends on a_1, a_2, and γ_f. Power allocation coefficients played a vital role in the ergodic rate of the far users. Therefore, when current techniques cannot perfectly remove the impact of HIs and ICSI, the SWIPT-assisted adaptive NOMA/OMA system with user selection has great potential for 5G communication networks and beyond. Appropriate target rate and power allocation coefficients can significantly improve the system performance without increasing the transmission power.

ACKNOWLEDGMENT

This research was supported by the National Natural Science Foundation of China under Grants 61801281 and 62171265.

CONFLICT OF INTEREST

The authors declare that there are no conflicts of interest.

ORCID

Jing Guo https://orcid.org/0000-0001-6688-9242

REFERENCES

1. Y. Saito, A. Benjebbour, Y. Kishiyama, and T. Nakamura, *System-level performance evaluation of downlink non-orthogonal multiple access (NOMA)*, (System-level performance evaluation of downlink non-orthogonal multiple access, London, UK), 2013, pp. 611–615.
2. Z. Ding, Z. Yang, P. Fan, and H. V. Poor, *On the performance of non-orthogonalmultiple access in 5G systems with randomly deployed users*, IEEE Signal Process. Lett. **21** (2014), no. 12, 1501–1505.
3. Z. Ding, M. Peng, and H. V. Poor, *Cooperative non-orthogonal multiple access in 5G systems*, IEEE Commun. Lett. **19** (2015), no. 8, 1462–1465.
4. T. Manimekalai, S. Joan, and T. Laxmikandan, *Throughput maximization for underlay CR multicarrier NOMA network with cooperative communication*, ETRI J. **42** (2020), no. 6, 846–858.
5. L. R. Varshney, *Transporting information and energy simultaneously*, (Proc. IEEE International Symposium on Information Theory, Toronto, Canada), 2008, pp. 1612–1616.
6. A. A. Nasir, X. Zhou, S. Durrani, and R. A. Kennedy, *Relaying protocols for wireless energy harvesting and information processing*, IEEE Trans. Wirel. Commun. **12** (2013), no. 7, 3622–3636.
7. Y. Xu, S. Chao, Z. Ding, X. Sun, Y. Shi, Z. Gang, and Z. Zhong, *Joint beamforming and power splitting control in downlink cooperative SWIPT NOMA systems*, IEEE Trans. Signal Process. **65** (2017), no. 18, 4874–4886.
8. A. K. Shukla, S. Vibhum, P. Upadhyay, A. Kumar, and J. Moualeu, *Performance analysis of energy harvesting-assisted overlay cognitive NOMA systems with incremental relaying*, IEEE Open J. Commun. Soc. **2** (2021), 1558–1576.
9. Z. Chen, Z. Ding, X. Dai, and R. Zhang, *An optimization perspective of the superiority of 5G NOMA compared to conventional OMA*, IEEE Trans. Signal Process. **65** (2017), 5191–5202.
10. W. Shin, M. Vaezi, B. Lee, D. Love, J. Lee, and H. V. Poor, *Nonorthogonal multiple access in multi-cell networks: Theory, performance, and practical challenges*, IEEE Commun. Mag. **55** (2016), no. 10, 176–183.
11. Y. Liu, Z. Ding, M. Elkashlan, and H. V. Poor, *Cooperative nonorthogonal multiple access with simultaneous wireless information and power transfer*, IEEE J. Sel. Areas Commun. **34** (2016), no. 4, 938–953.
12. N. Nomikos, T. Charalambous, D. Vouyioukas, G. K. Karagiannidis, and R. Wichman, *Hybrid NOMA/OMA with buffer-aided relay selection in cooperative networks*, IEEE J. Sel. Top. Signal Process. **13** (2019), no. 4, 938–953.
13. E. Costa and S. Pupolin, *M-QAM-OFDM system performance in the presence of a nonlinear amplifier and phase noise*, IEEE Trans. Commun. **50** (2002), no. 3, 462–472.
14. S. Solanki, V. Singh, and P. K. Upadhyay, *RF energy harvesting in hybrid two-way relaying systems with hardware impairments*, IEEE Trans. Vehic. Technol. **68** (2019), no. 12, 11792–11805.
15. X. Li, J. Li, Y. Liu, Z. Ding, and A. Nallanathan, *Residual transceiver hardware impairments on cooperative NOMA networks*, IEEE Trans. Wirel. Commun. **19** (2020), no. 1, 680–695.
16. D. W. K. Ng, E. S. Lo, and R. Schober, *Robust beamforming for secure communication in systems with wireless information and power transfer*, IEEE Trans. Wirel. Commun. **13** (2014), no. 8, 4599–4615.
17. X. Li, J. Li, and L. Li, *Performance analysis of impaired SWIPT NOMA relaying networks over imperfect Weibull channels*, IEEE Syst. J. **14** (2020), no. 1, 669–672.
18. A. Celik, M. Tsai, R. M. Radaydeh, F. S. Al-Qahtani, and M. Alouini, *Distributed user clustering and resource allocation for imperfect NOMA in heterogeneous networks*, IEEE Trans. Commun. **67** (2019), 7211–7227.
19. D. S. W. Hui and V. K. N. Lau, *Design and analysis of delay-sensitive cross-layer OFDMA systems with outdated CSIT*, IEEE Trans. Wirel. Commun. **8** (2009), no. 7, 3484–3491.
20. T. Schenk, *RF Imperfections in high-rate wireless systems: impact and digital compensation*, Springer, New York, 2008.
21. Y. Zeng and R. Zhang, *Full-duplex wireless-powered relay with selfenergy recycling*, IEEE Wirel. Commun. Lett. **4** (2015), no. 2, 201–204.
22. D. P. M. Osorio, E. E. B. Olivo, H. Alves, J. C. S. S. Filho, and M. Latva-aho, *Exploiting the direct link in full-duplex amplify-and-forward relaying networks*, IEEE Signal Process. Lett. **22** (2015), no. 10, 1766–1770.
23. X. Yue, Y. Liu, S. Kang, A. Nallanathan, and Z. Ding, *Exploiting full/half-duplex user relaying in NOMA systems*, IEEE Trans. Commun. **66** (2018), no. 2, 560–575.

24. V. N. Q. Bao, H. Y. Kong, and S. W. Hong, *Performance analysis of M-PAM and M-QAM with selection combining in independent but non-identically distributed Rayleigh fading paths*, (Proc. IEEE 68th Vehicular Technology Conference, Calgary, Canada), 2008, pp. 1–5.
25. J. L. Vicario and C. Anton-Haro, *Analytical assessment of multi-user vs. spatial diversity trade-offs with delayed channel state information*, IEEE Commun. Lett. **10** (2006), no. 8, 588–590.
26. I. S. Gradshteyn and I. M. Ryzhik, *Table of integrals, series and products*, 7th ed., Academic Press, New York, 2007.
27. A. P. Prudnikov, Y. A. Brychkov, and O. I. Marichev, *Integrals and series (special functions)*, Gordon and Breach, New York, 1986.
28. N. C. Beaulieu and J. Hu, *A closed-form expression for the outage probability of decode-and-forward relaying in dissimilar Rayleigh fading channels*, IEEE Commun. Lett. **10** (2006), no. 12, 813–815.
29. K. Reshma and A. Babu, *Throughput analysis of energy harvesting enabled incremental relaying NOMA system*, IEEE Commun. Lett. **24** (2020), no. 7, 1419–1423.

AUTHOR BIOGRAPHIES

Jing Guo received the Ph.D. degree in Communication and Signal Processing with the State Key Laboratory of Integrated Services Networks, Xidian University, Xi'an, China. She is currently a lecturer of the School of Electronic Information and Artificial Intelligence, Shaanxi University of Science & Technology, Xian, Shaanxi, China. Her current research interests include NOMA cooperative systems, reconfigurable intelligent surface (RIS), and wireless communication theory.

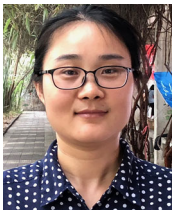

Jin Lu received the B.E., M.E., and Ph.D. degrees in Signal and Information Processing from Xidian University, Xi'an, China, in 2007, 2010, and 2014, respectively. She is currently a lecturer of the School of Electronic Information and Artificial Intelligence, Shaanxi University of Science and Technology, Xian, Shaanxi, China. Her research interests include estimation, tracking, and signal processing, with an emphasis on weak target detection and tracking.

Xianghui Wang received the bachelor's degree in Electronics and Information Engineering from the Xi'an University, Xi'an, China, in 2008; the master's degree in Signal and Information Processing from the Northwestern Polytechnical University (NPU), Xi'an, China, in 2011; and the Ph.D. degree in Information and Communication Engineering from the NPU in 2020. He was also a visiting Ph.D. student at the the Andrew and Erna Viterby Faculty of Electrical Engineering, Technion—Israel Institute of Technology, Haifa, Israel, between 2016 and 2018. He is currently a lecturer of the School of Electronic Information and Artificial Intelligence, Shaanxi University of Science and Technology, Xian, Shaanxi, China. His research interests include speech enhancement and microphone array signal processing.

Lili Zhou received her B.S. and M.S. degrees in Communication and Information Systems from Xi'an University of Technology, Xi'an, China, in 2004 and 2007, respectively, and her Ph.D. degree in Electronic Science and Technology from Xi'an University of Technology, Xi'an, China, in 2011. She is currently an associate professor with the School of Electronic Information and Artificial Intelligence, Shaanxi University of Science and Technology, Xi'an, China. Her research interests include wave propagation and numerical calculation of electromagnetic fields.

How to cite this article: J. Guo, J. Lu, X. Wang, and L. Zhou, *Performance analysis of SWIPT-assisted adaptive NOMA/OMA system with hardware impairments and imperfect CSI*, ETRI Journal **45** (2023), 254–266. https://doi.org/10.4218/etrij.2021-0447